

PAPER • OPEN ACCESS

Effectiveness of dynamic induction control strategies on the wake of a wind turbine

To cite this article: M Montenegro Montero *et al* 2022 *J. Phys.: Conf. Ser.* **2265** 022054

View the [article online](#) for updates and enhancements.

You may also like

- [The errors in digital image correlation due to overmatched shape functions](#)
Liping Yu and Bing Pan
- [Digital image correlation with self-adaptive scheme for interpolation bias reduction](#)
Peihan Tu
- [Causes of increased dissolved inorganic carbon in the subsurface layers in the western shelfbreak and high latitudes basin in the Arctic Pacific sector](#)
Gangzhi Chu, Xiaofan Luo, Zijia Zheng et al.



*Benefit from connecting
with your community*

ECS Membership = Connection

ECS membership connects you to the electrochemical community:

- Facilitate your research and discovery through ECS meetings which convene scientists from around the world;
- Access professional support through your lifetime career;
- Open up mentorship opportunities across the stages of your career;
- Build relationships that nurture partnership, teamwork—and success!

Join ECS! **Visit electrochem.org/join**



Effectiveness of dynamic induction control strategies on the wake of a wind turbine

M Montenegro Montero, V Arcari, S Cacciola, A Croce

Dept. of Aerospace Science and Technology, Politecnico di Milano, via La Masa 34, 20156 Milano, Italy

Author contact email: mariana.montenegro@polimi.it

Keywords: Dynamic induction control, wind farm control, wake recovery, pitch collective motion, aeroelastic simulations.

Abstract

Dynamic Induction Control (DIC) has been recently proposed as means for enhancing wake recovery and, in turn, for increasing the overall produced power. A faster wake recovery is triggered by a Periodic Collective Motion (PCM), following a single sine function (S-PCM), or by a combination of Gaussian functions (G-PCM). Both techniques are associated with power gains in simple two- or three-turbine farms, but entail an increase in machine loading. A technique named the Helix approach generates a dynamic induction through a thrust that varies in direction but not in magnitude, reducing the tower loading. This work aims to analyse the impact of bluff bodies, such as nacelle and tower on the performances of PCD techniques, and to quantify the DIC impact on the loads. A 5 MW reference wind turbine is used for the model, implemented in OpenFAST and SOWFA to perform large-eddy simulations (LES). The results obtained at a distance of 3D downstream, show less evidence of the bluff bodies using the PCM than the baseline, as an effect of the increased in-wake mixing. In a two-turbine wind farm with a separation of 3D between turbines, this effect leads to an increment in the overall power output of the farm, despite the presence of the tower and nacelle. The blockage itself does not seem to hamper the effectiveness of DIC. In both cases, DIC is responsible for an increment of about 7% in the overall power output.

1 Introduction

Wind farm control is nowadays considered an established technique to increase the overall power output of a wind farm, through the reduction of the detrimental impact that wakes have on downstream machines. Dynamic Induction Control (DIC) has been recently proposed as means for enhancing wake recovery and, in turn, for increasing the overall produced power. By using this control method, the induction factor of an upstream wind turbine varies over time, incurring in wake mixing that allows a downstream turbine to have better power production as it experiences higher wind velocities. According to DIC, a faster wake recovery is triggered by either a Periodic Collective Motion (PCM) or a Dynamic Individual Pitch Control (DIPC). In literature, two versions of PCM have been tested. The first is based on a collective pitch motion following a single sine function (S-PCM), whose frequency is chosen to boost the wake recovery mechanism. Sinusoidal input signals on the blades' pitch were shown to cause the quasi-periodic shedding of vortex rings when using an optimal parameter for the total production of the 4x4 wind farm of $St = 0.25$ and could increase power production up to 6%, according to Munters and Meyers [1]. The percentage increase in the power production of small wind farms is also observed both in numerical simulations and in wind tunnel experiments. A second version of the PCM is based on a more complex collective pitch function made by a combination of Gaussian functions (G-PCM), which is more efficient than S-PCM in accelerating the wake recovery, especially in the



near wake region [2]. Both techniques are associated with a small percentage gain in power in simple two- or three-turbine farms, but entail an increase in ultimate and fatigue loading on the machine. In an attempt to overcome this issue, a particular DIPC technique named the Helix approach has been proposed [3], which via a dedicated transformation generates a dynamic induction through a thrust that varies in direction but not in magnitude, reducing the tower loading.

In the CFD simulations on which most of the results of the aforementioned works are based, the turbines are rendered through the sole blades, neglecting the presence of bluff bodies as nacelle and tower. This may not be relevant for power production or torque, but it does delay vortex breakdown as it stabilises the wake [4]. This point deserves special attention. In fact, even if the tower and nacelle do not contribute much to a single isolated turbine power production, they significantly influence the wake kinetic energy and symmetry [5]. It has been demonstrated that in the near wake, a downstream turbine sees important changes in power, thrust and wake profile when the bluff bodies are considered [6].

2 Objective

The main objective of this work is to analyse the impact the bluff bodies such as the tower and nacelle have on the wake of a turbine. The performance of S-PCM and G-PCM are compared against a baseline case, considering the bluff bodies, in an LES environment. Moreover, single wind turbine analyses are performed with the purpose of evaluating the influence of helix DIPC on the turbine's aeroelastic response.

3 Methodology

The model of the 5 MW reference wind turbine, provided by the National Renewable Energy Laboratory (NREL) [7] was implemented in OpenFast and included in the SOWFA environment, to perform all LES simulations. It consists of an up-wind three-bladed, 126 m diameter rotor mounted on top of an 87.6 m tower. The turbine model is linked to a reference controller based on a generator-torque controller and a full-span rotor-collective blade pitch controller, which operate independently from each other. Below rated the generator-torque controller is designed to maximize power production, whereas the collective blade pitch controller is used above rated for regulating the generator speed. This is taken as the baseline control for the cases in this work.

The periodic collective pitch of the blades is achieved through the implementation of the desired movements into the turbine controller. The baseline controller of the turbine was modified in order to impose the sinusoidal motion of the blade pitch angles as shown in Eq. 1.

$$\beta_{\text{SPCM}} = \beta_{\text{trim}} + A_{\text{PCM}} \sin(2\pi f_{\text{PCM}}t + \phi_{\text{SPCM}}) \quad (1)$$

In the equation β_{trim} is the pitch angle from the baseline controller, A_{PCM} is the amplitude of the periodic DIC motion, f_{PCM} is the frequency, while ϕ_{PCM} is the phase used to ensure a smooth activation of the control. In all the simulations, amplitude A_{PCM} was set equal to 2.5° and the frequency f_{PCM} to 0.026 Hz, corresponding to Strouhal number of 0.36, which resulted in the optimal range for overall power increase in previous works [8].

The Gaussian PCM control [9], instead, emphasises the SPCM mixing phenomenon. This effect is accomplished by designing a periodic asymmetric control law, characterised by higher positive peaks (reduction of collective incidence angle) with respect to negative ones. Additionally, to maintain average blade operation around the optimal angle of attack, negative portions of the signal are more dilated with respect to positive ones, achieving a zero mean pitch. Thus, a sum of two reversed Gaussian functions control peak separation and amplitude. The G-PCM control law is defined in Eq. 2.

$$\beta_{\text{GPCM}} = \beta_{\text{trim}} + A_{\text{PCM}} \frac{(g_1(x) + g_2(x) - C) \sin^\xi(\pi x)}{\beta_{\text{max}}} \quad (2)$$

Here, $g_1(x)$ and $g_2(x)$ are the Gaussian functions, x is the normalised time, β_{max} is the higher positive peak and ξ is a smearing factor. The shape of β_{GPCM} , along with the pitch cycles of the other methods studied, can be visualized in Figure 1a.

The Helix approach [3] is a Dynamic Individual Pitch Control (DIPC) that uses a modified version of the multi-blade coordinate (MBC) transformations to achieve periodic yaw and tilt moments on the turbine. The wake is manipulated, slowly changing its direction over time, increasing wake-mixing to boost the power production of the downstream turbines with minimal rotor thrust fluctuations. In other words, the objective of the helix method is to achieve a varying tilt and yaw moment on the turbine to induce a varying directional thrust force, thanks to a super-imposed sinusoidal excitation on the blades' pitch angle, out of phase by 120 degrees between them. At a given time, the blades are loaded differently according to their azimuth position. Figure 1b shows the three control laws for the blade pitch.

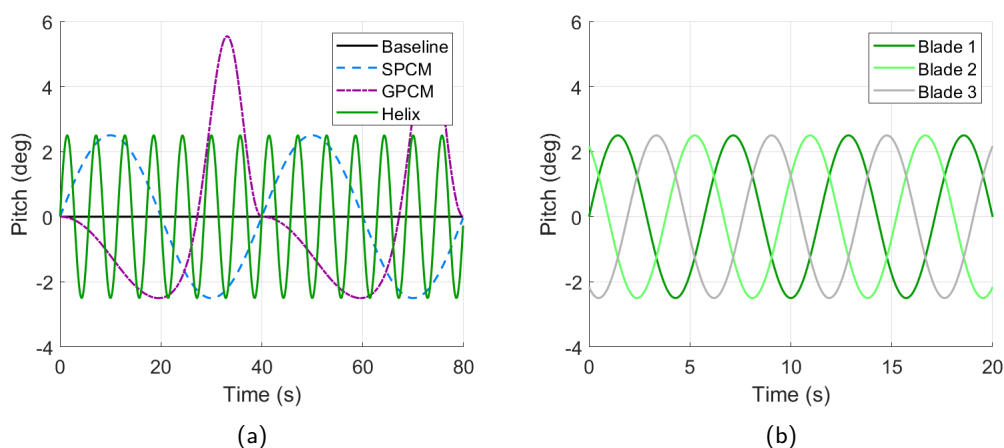


Figure 1: (a) Pitch cyclic motion of one blade under different pitch control methods. (b) Individual pitch control with Helix method.

An LES approach has been chosen for simulating the turbulent ABL inflow consists in running two distinct analyses with different SOWFA applications. The computational domain is a box of 3 km \times 3 km \times 1 km. The second turbine is placed three diameters (3D) downstream from the first one, closer than the usual placing, as previous analyses of the G-CPM method for this turbine showed that at this distance the wake presented the highest percentage of velocity gain in the wake (14%) [2]. The nacelle is integrated into the computation domain as a cylindrical body elongated in the downwind direction. Additionally, the hub is modelled as a simple static sphere fused directly to the nacelle. Both bluff bodies have the same radius of two meters, and the nacelle has a length of 10 m. The hub is positioned at an elevation of 90 m above the ground. The tower aerodynamics has been rendered through a standard lifting line. The nacelle and hub have been meshed and directly integrated into the computational domain. All simulations refer to a wind speed of 9 m/s and roughness length equal to 0.003 m.

The control strategies are implemented in OpenFAST through a dynamic link library (DLL) which allows for the independent blade pitch motions. All aeroelastic simulations were performed for 600 s with a time-step of 0.016 s, which resulted adequate to model the physics of interest and ensure the stability of the computation.

4 Results

Single wind turbine LES analyses were performed to study the impact of bluff bodies on the free wake. The near/wake flow in the tower symmetry plane was studied using the mean velocity field, time-averaged over ten PCM periods. Figure 2 compares the velocity deficit profile of the Baseline simulation with and without the bluff bodies at different stream-wise locations, where the full lines and the dashed lines represent the cases with and without nacelle and tower, respectively. The horizontal dashed lines indicate the location of the top blade tip and the bottom blade tip. The case with the nacelle clearly experiences a bigger loss at the rotor

center due to the blockage created by the nacelle. However, it is possible to see that the effect the bluff bodies have over the wake recovery lessens in the near wake, although it remains visible also at 7 diameters.

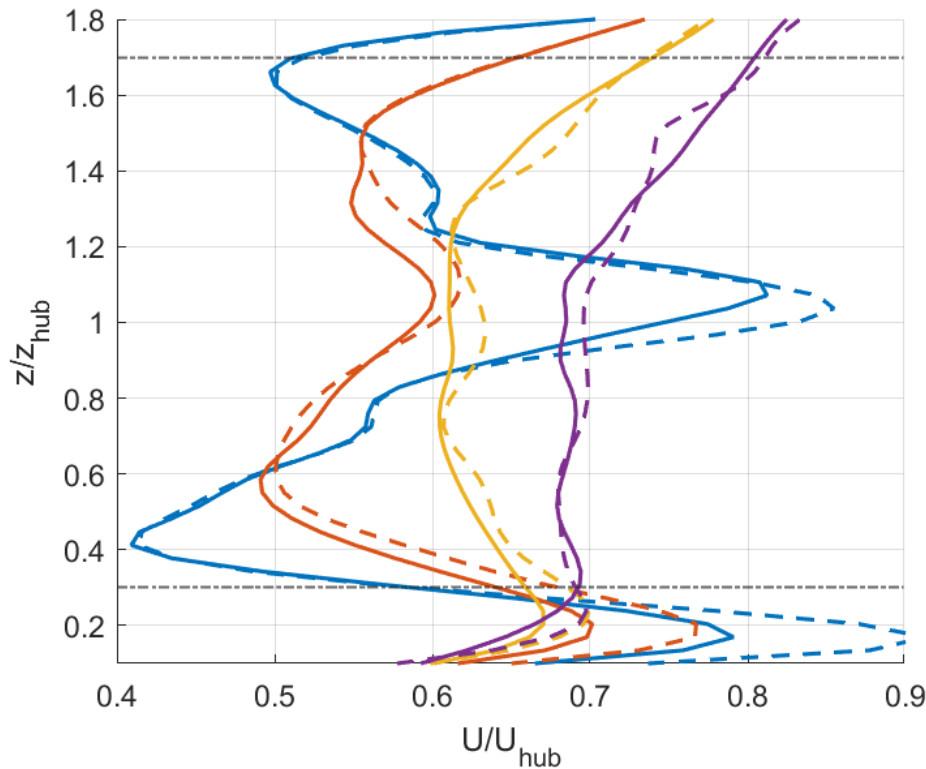


Figure 2: Wind speed profiles at different stream-wise locations behind the turbine: one diameter (blue), three diameters (orange), five diameters (yellow), seven diameters (purple). Solid lines show the cases with nacelle and tower present. Dashed lines show cases without bluff bodies.

Table 1 shows the mean percentage difference between the flow velocity with and without tower and nacelle. The negative values indicate that there is a lower velocity in the simulation with the bluff bodies. Previous analysis has shown the PCM techniques are associated with an increased average flow velocity in the wake. In particular, the Gaussian control has the most significant increments, reaching a maximum velocity percentage gain of 14.28% in the wake, compared to the Baseline control. Now, even though the missing structures such as nacelle and tower have been inserted, the G-PCM and S-PCM controls always exhibit an increment in the average speed in the wake compared to the Baseline case, with a maximum percentage gain of 14.42% and 7.71% respectively, confirming that the G-PCM logic remains the most effective in terms of re-energisation. The PCM logics have a more important effect at three rather than at five diameters. It seems that inside the near wake of the upwind rotor, induction effects from large PCM eddies, which are observed from 2 to 5 diameters downstream of the PCM-equipped machine, are fully exploited. This is confirmed in particular for G-PCM control, which is observed to produce an important recovery with respect to the S-PCM strategy, especially at three diameters.

Looking at the contours and at the $x - y$ plane (Figures 3 to 5), the velocity field on the symmetry plane highlights a prominent high-speed flow region behind the rotor hub, with a stronger velocity deficit behind the blades. This near-wake flow pattern is associated with a reduction in lift, and correspondingly axial induction, at the blade roots [10]. The high-speed region is pressing immediately behind the nacelle but quickly disappears as it proceeds downstream. What immediately jumps out is that the high-speed zone, with activated PCM controls, disappears already three diameters away, giving a more uniform speed distribution over the rotor area, while in the Baseline it is still present. The effects of the nacelle and the tower are evident above all at a one distance diameter: for the G-PCM, there is a reduction of the velocity magnitude in the percentage of

Table 1: Wake average velocities at different stations and percentage loss difference.

Baseline				
	1D	3D	5D	7D
\bar{u} (with bluff bodies) [m/s]	4.66	5.27	6.14	6.70
\bar{u} (without bluff bodies) [m/s]	4.72	5.32	6.18	6.77
$\Delta\bar{u}$ [%]	-1.27	-0.94	-0.65	-1.03
S-PCM				
	1D	3D	5D	7D
\bar{u} (with bluff bodies) [m/s]	4.76	5.69	6.54	7.02
\bar{u} (without bluff bodies) [m/s]	4.81	5.74	6.57	7.03
$\Delta\bar{u}$ [%]	-1.27	-0.87	-0.46	-0.14
G-PCM				
	1D	3D	5D	7D
\bar{u} (with bluff bodies) [m/s]	5.01	6.03	6.67	7.09
\bar{u} (without bluff bodies) [m/s]	5.06	6.08	6.70	7.11
$\Delta\bar{u}$ [%]	-0.98	-0.82	-0.45	-0.28

-10%, and for the S-PCM it even reaches -12%. For the Baseline control, it comes to -15%, which emphasises the effectiveness of applying an active control on the blades to allow a better and earlier re-energization of the wake and reducing the velocity deficit from the outer flow. However, the influence of bluff bodies, with dynamic PCM logics, already vanishes at three diameters away and shows almost zero difference compared to cases without bluff bodies at five and seven diameters out. The same cannot be said for the Baseline case, where the footprint of the tower and nacelle clearly persists up to five diameters. The figures also show that the near-wake of the bluff bodies is shifted to the left; that is a consequence of the swirl in the wake as it rotates in the opposite direction of the rotor blades, due to the conservation of the angular momentum.

As expected, the presence of the nacelle and tower is strongly visible in the wake at 1D, entailing a reduction of velocity up to 10%. Again at 1D, the presence of the farm control does not modify significantly the in-wake speed. The results at 3D, on the other hand, are more interesting. In fact, while in the baseline some residuals of the nacelle and tower blockage remain, in the S-PCM case their fingerprint is present but strongly reduced as an effect of the increased in-wake mixing.

Next, one turbine was studied using the Helix approach. The analyses conducted were done directly in OpenFAST without going through a CFD simulation, allowing to quickly analyse if the controller is correctly implemented and obtain an initial estimate of the power produced, thrust, deflection, loads, and oscillations. Without using SOWFA, the inlet wind was calculated directly by InflowWind. It is a methodology closer to the wake-redirection family, as the wake is dynamically manipulated and deviated from the path it would generally follow. This is done thanks to the cyclic pitching that, by changing the azimuthal loading on the disk, creates a significant tilting of the axial induction plane. The simulations had the uniform inlet wind with reference speed at 9 m/s, therefore with zero turbulence and a constant velocity profile across the height. The excitation

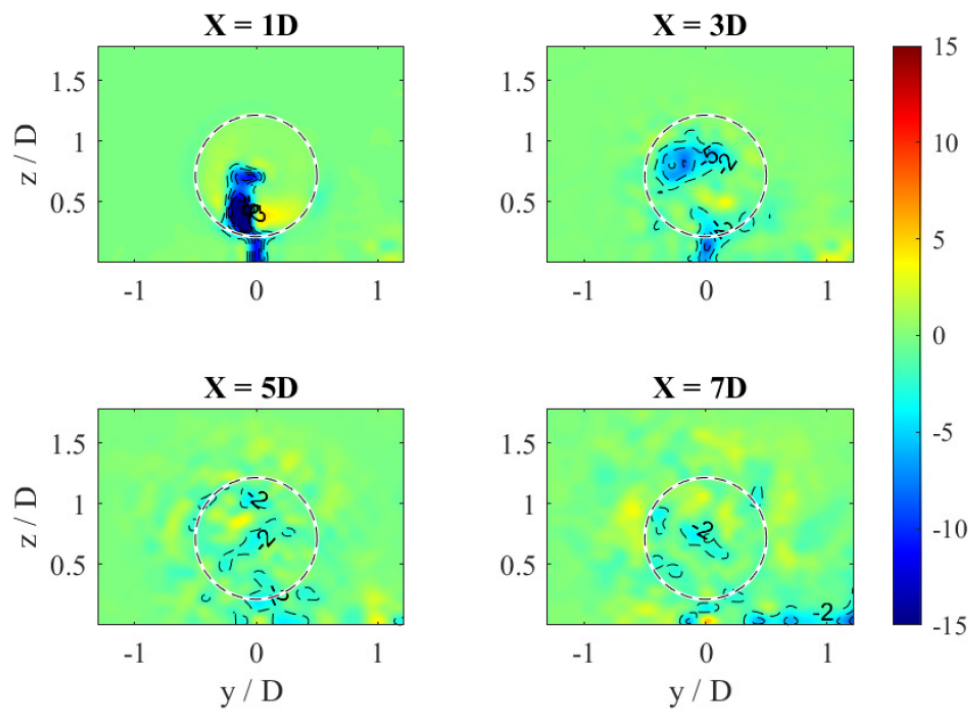


Figure 3: Contour in the $y - z$ plane of the percentage loss of speed in the wake due to the presence of the nacelle and tower structures, Baseline.

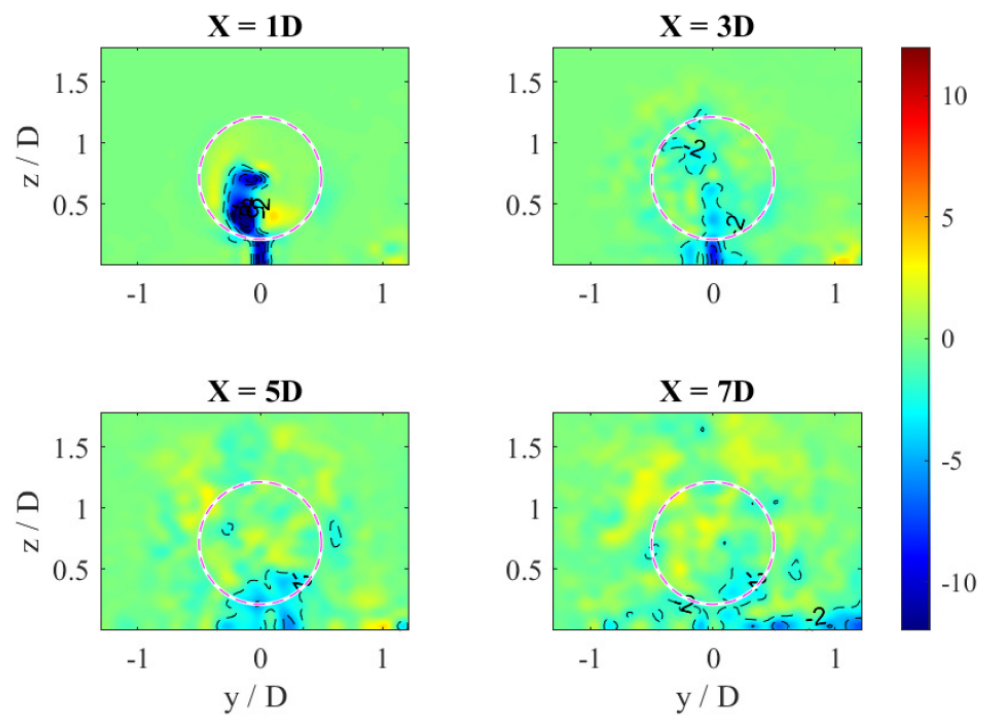


Figure 4: Contour in the $y - z$ plane of the percentage loss of speed in the wake due to the presence of the nacelle and tower structures, S-PCM.

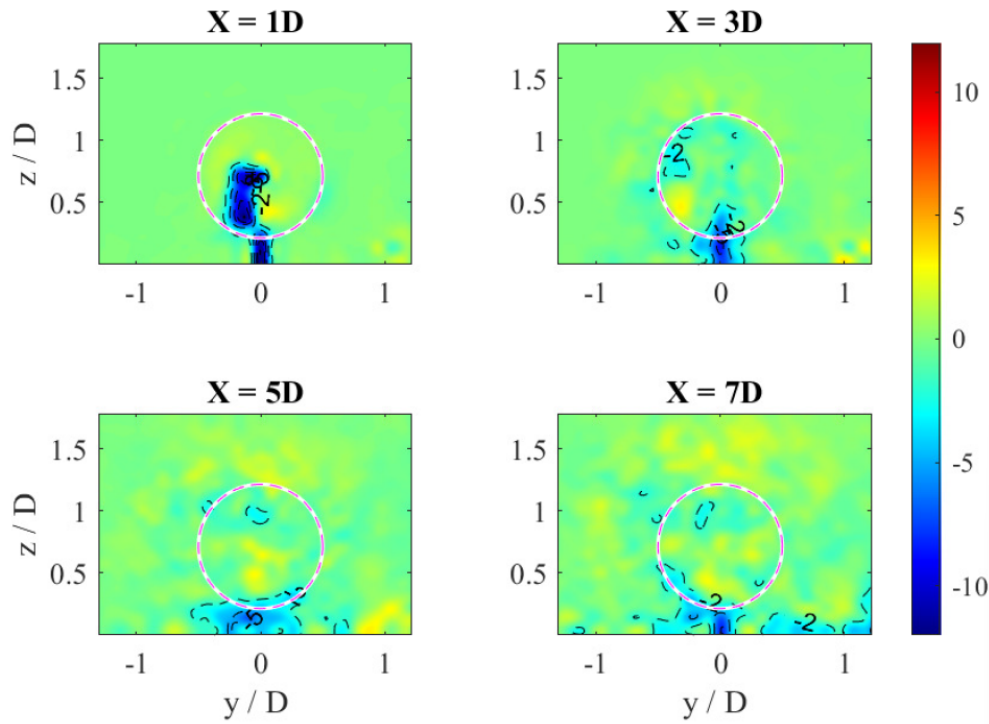


Figure 5: Contour in the $y - z$ plane of the percentage loss of speed in the wake due to the presence of the nacelle and tower structures, G-PCM.

frequency f_e was identical to the PCM cases, that is, $St = 0.36$ ($f_e = 0.025 \text{ Hz}$).

Table 2 shows the results for power, thrust, torque and rotor speed with uniform inlet wind at 9 m/s. The helix approach presents a good average power output comparable to that of the S-PCM, with a percentage loss of 2.61% compared to the baseline control. There is a slight percentage loss for the thrust, always with respect to baseline, by 0.95%. The results obtained for the G-PCM confirm what was seen in the CFD simulations presented earlier. This control has the most significant percentage deficit on the average power produced: 4.85% compared to the baseline case. The time histories of these quantities are shown in Figure 6.

Table 2: Rotor power, rotor speed, thrust and generator torque average values with uniform wind (reference wind speed of 9 m/s) for different wind farm control laws.

	BASELINE	S-PCM	G-PCM	HELIX
Power [kW]	2504.4	2442.4	2382.9	2438.1
Rot. speed [rpm]	10.1	10.0	9.5	10.0
Thrust [kN]	547.1	542.4	529.3	541.9
Gen. torque [kNm]	24.5	24.1	24.9	24.0

Now a question arises over the potential impact of such bluff bodies on the performance of DIC in terms of overall power production. In fact, although the DIC eases the dissolution of bluff body blockage, the presence of the tower and nacelle may interact with the fluid-dynamics mechanism that DIC exploits to strengthen the

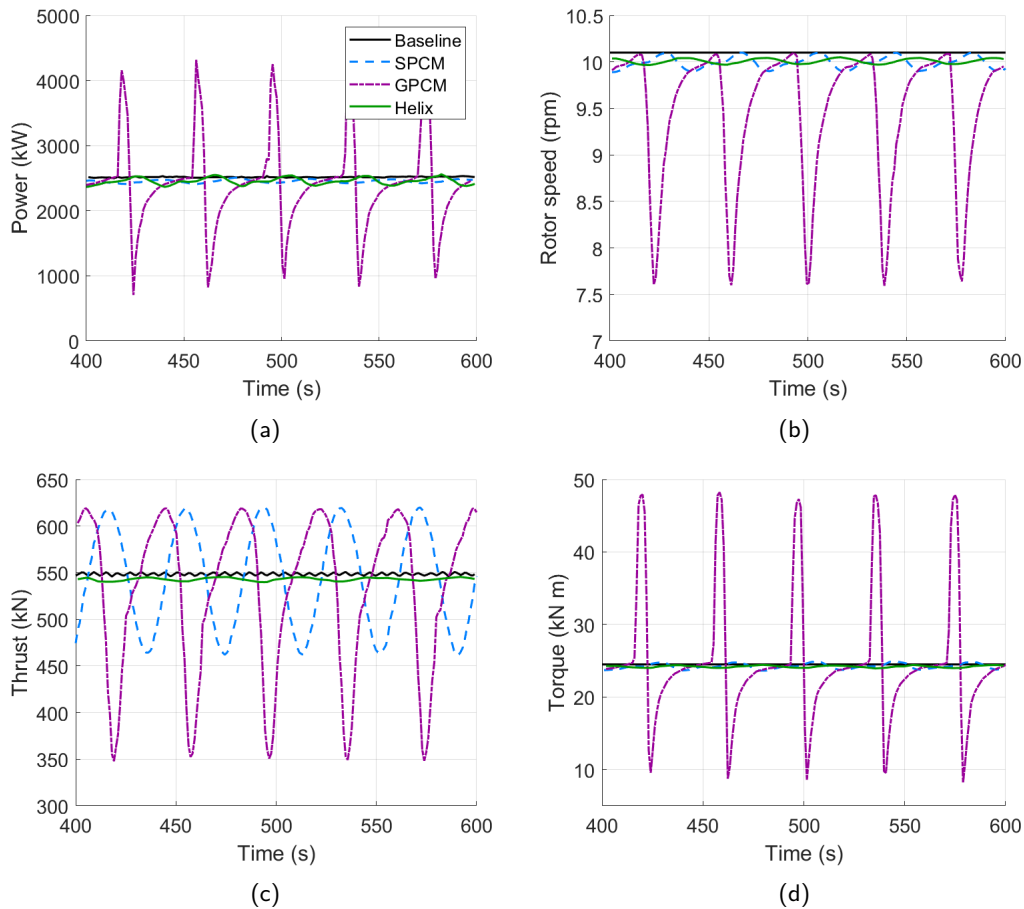


Figure 6: Rotor power (a), rotor speed (b), thrust (c) and generator torque (d) time histories with uniform wind for different wind farm control laws.

wake recovery. The method used for this was the G-PCM.

To this end, a set of simulations with a simple two-turbine wind farm has been performed. The turbines are separated by 3D to accentuate the mutual interaction among wake, DIC and bluff bodies. Table 3 summarises the overall power produced by this simple wind farm in four different cases (with and without bluff bodies and DIC). Looking at the difference between the cases with and without bluff bodies (Tab. 3, last column), one can readily verify that the presence of tower and nacelle blockage is detrimental, as expected, entailing a small percentage of total power losses. However, the blockage itself does not seem to hamper the effectiveness of DIC. In fact, in both cases, DIC is responsible for an increment of about 7% in the overall power output (Tab. 3, last row). This result has great value as it demonstrates how the decrease in the average speed of the wake, albeit small, linked to the presence of the structures, dramatically influences the power production of the downstream machine.

5 Conclusions

This work presented the results of LES-based analyses, aimed at evaluating the effectiveness of different dynamic induction controls when the presence of tower and nacelle is considered in the simulation domain. It considered a sinusoidal PCM and a Gaussian PCM approach and the impact the presence of bluff bodies (i.e. tower and nacelle) has on their performance. From the obtained results, we can assess that, despite the presence of nacelle and tower, which increases the velocity deficit in the wake, the PCM controls prove to be very effective in re-energizing the wake as a very significant speed increase is obtained compared to the

Table 3: Overall power produced by a two-turbine farm at 9 m/s and roughness length $z_0 = 0.003$ m.

	w/o bluff bodies	w/ bluff bodies	Difference [%]
Nominal farm [kW]	3500	3359	-4.05
DIC control [kW]	3748	3596	-4.1
Gain [%]	7.10	7.05	

baseline case.

The impact of the nacelle and tower was evaluated on the power production of the downstream turbine. The presence of the structures results in an important negative influence on the power production of the downstream machine. When looking at the overall power production, there was still an increase with respect to the power production with no PCM control, demonstrating that under more realistic conditions, the DIC is still improving the wake recovery. Despite the negative contribution of the bluff bodies to the power production of a single isolated turbine, present results show that they influence the wake dynamics significantly. The analyzed dynamic induction control techniques remain effective in increasing the farm power output also if tower and nacelle interference are included in the simulation. Therefore, when an array of turbines is considered, modelling tower and nacelle provides a more realistic inflow for waked turbines due to the more accurate calculation of the wake recovery and entrainment. This is very important when the performances of the entire array are considered. The asymmetry in the velocity may induce fatigue loads on waked turbines that drastically differ from those that would be computed neglecting the presence of tower and nacelle.

The Helix approach applied to the isolated upstream turbine presents an acceptable average power output compared to the S-PCM, with a percentage loss of 2.61% compared to the Baseline control. Further work needs to be done to evaluate the impact of DICP on turbine and farm levels, allowing for a thorough comparison with S-PCM and G-PCM.

Acknowledgements

We acknowledge the CINECA award under the ISCRA initiative, for the availability of high-performance computing resources and support.

This project has received funding from the European Union's Horizon H2020 research and innovation programme under the Marie Skłodowska-Curie grant agreement N°860579.

References

- [1] W. Munters and J. Meyers. Towards practical dynamic induction control of wind farms: Analysis of optimally controlled wind-farm boundary layers and sinusoidal induction control of first-row turbines. *Wind Energy Science*, 3(1):409–425, 2018.
- [2] A. Croce, S. Cacciola, R. Praticó, V. Acari, and M. Montenegro Montero. Exploiting vortex roll-up mechanism to promote wake recovery through a periodic and asymmetric collective pitch motion. *Wind Energy Science Conference*, Hannover, Germany, 2021.
- [3] J. A. Frederik, B. M. Doekemeijer, S. P. Mulders, and J. Wingerden. The helix approach: Using dynamic individual pitch control to enhance wake mixing in wind farms. *Wind Energy*, 23(8):1739–1751, 2020.
- [4] A. Abraham, T. Dasari, and J. Hong. Effect of turbine nacelle and tower on the near wake of a utility-scale wind turbine. *Journal of Wind Engineering and Industrial Aerodynamics*, 193:103981, 2019.

- [5] Christian Santoni, Kenneth Carrasquillo, Isnardo Arenas-Navarro, and Stefano Leonardi. Effect of tower and nacelle on the flow past a wind turbine. *Wind Energy*, 20(12):1927–1939, 2017.
- [6] J. Wang, D. McLean, F. Campagnolo, T. Yu, and C. L. Bottasso. Large-eddy simulation of waked turbines in a scaled wind farm facility. *Journal of Physics: Conference Series*, 854:012047, 2017.
- [7] J. Jonkman, S. Butterfield, W. Musial, and G. Scott. Definition of a 5-mw reference wind turbine for offshore system development. 2009.
- [8] J. A. Frederik, R. Weber, S. Cacciola, F. Campagnolo, A. Croce, C. Bottasso, and J.-W. van Wingerden. Periodic dynamic induction control of wind farms: proving the potential in simulations and wind tunnel experiments. *Wind Energy Science*, 5(1):245–257, 2020.
- [9] A. Croce, M. Cacciola, S. and Montenegro Montero, R. Praticó, and V. Acari. A cfd-based analysis of dynamic induction techniques for wind farm control applications. *Wind Energy*, WE-22-0013, under review, 2022.
- [10] M. Magnusson. Near-wake behaviour of wind turbines. *Journal of Wind Engineering and Industrial Aerodynamics*, 80(1-2):147–167, 1999.